Applied Radiation and Isotopes 109 (2016) 544–546

Contents lists available at ScienceDirect

Applied Radiation and Isotopes

journal homepage: www.elsevier.com/locate/apradiso

A prototype of radioactive waste drum monitor by non-destructive assays using gamma spectrometry

Tran Thien Thanh [a,b,*], Hoang Thi Kieu Trang [a,b], Huynh Dinh Chuong [b], Vo Hoang Nguyen [a], Le Bao Tran [a,b], Hoang Duc Tam [a,c], Chau Van Tao [a,b]

[a] Department of Nuclear Physics, Faculty of Physics and Engineering Physics, VNUHCM-University of Science, 227, Nguyen Van Cu Street, District 5, Ho Chi Minh City, Vietnam
[b] Nuclear Technique Laboratory, VNUHCM-University of Science, 227, Nguyen Van Cu Street, District 5, Ho Chi Minh City, Vietnam
[c] Faculty of Physics, Ho Chi Minh City University of Pedagogy, 280, An Duong Vuong Street, District 5, Ho Chi Minh City, Vietnam

HIGHLIGHTS

- Segmented gamma scanning and gamma emission tomography are used to locate point source in waste drums.
- The PENELOPE software is used to compute the detection efficiency of the localized point source in the waste drum.
- The activity of ^{137}Cs and ^{60}Co point source could be determined with an accuracy better than 10% for air and sand matrices.

ARTICLE INFO

Article history:
Received 28 March 2015
Accepted 19 November 2015
Available online 29 November 2015

Keywords:
Segmented gamma scanning
Gamma emission tomography
Waste drum
Point spread function

ABSTRACT

In this work, segmented gamma scanning and the gamma emission tomography were used to locate unknown sources in a radioactive waste drum. The simulated detector response function and full energy peak efficiency are compared to corresponding experimental data and show about 5.3% difference for an energy ranging from 81 keV to 1332.5 keV for point sources. Computation of the corresponding activity is in good agreement with the true values.

1. Introduction

Radioactive waste management requires that the composition of radioactive isotopes and their activities in waste drums must be characterized in order to verify its compliance with the national regulations for intermediate storage or final disposal. The radioactive waste can be in liquid, solid or gas form. Each type has distinct characteristics and requires appropriate treatments. Segmented gamma scanning (SGS) is one of the most widely applied non-destructive analytical techniques to characterize radioactive waste drums. In this technique, the activity concentration is generally calculated assuming a homogeneous material and activity distribution for each measured drum segment. However, real radioactive waste drums exhibit non-uniform density and radionuclides distributions that strongly affect the reliability and accuracy of activity results in SGS. In recent years, (Bai et al., 2009; Krings and Mauerhofer, 2011, 2012; Gurau and Sima, 2012) research involved improving the accuracy of measured activity even with heterogeneous distributions of material and radionuclides in the waste drums.

In this work, we focus on improving the accuracy of the location of radioactive sources and the waste drum activity by combining gamma emission tomography with the SGS technique based on a NaI(Tl) detector. The tomographic image is reconstructed based on the filtered back-projection method. The experimental efficiency calibration has been established for the NaI(Tl) detector. The simulated full energy peak efficiencies are used to calculate activities of radiation sources inside waste drums. The measurement results are compared to the true activity data and reveal some discrepancies that are also discussed.

2. Materials and methods

2.1. Experimental set-up

A standard drum of 210 L volume, 58 cm in diameter, 86 cm high, containing a sand matrix, is placed at a distance of 6.3 cm

* Corresponding author at: Department of Nuclear Physics, Faculty of Physics and Engineering Physics, VNUHCM-University of Science, 227, Nguyen Van Cu Street, District 5, Ho Chi Minh City, Vietnam.
E-mail address: ttthanh@hcmus.edu.vn (T.T. Thanh).

http://dx.doi.org/10.1016/j.apradiso.2015.11.037
0969-8043/

from a NaI(Tl) detector. A collimator consisting of a hollow lead cylinder of 15 cm length, 9.5 cm inner diameter and 10.5 cm outer diameter completely surrounds the detector. The NaI(Tl) detector is connected to the Osprey™ (Canberra, 2014) tube which is a high-performance, fully integrated multi-channel analyzer (MCA) tube base that contains everything needed to support scintillation spectrometry. This compact unit contains a high-voltage power supply (HVPS), preamplifier, and a full featured digital MCA. It can be controlled with only one cable from the Osprey™ to the control and data acquisition system. Acquisitions of photon spectra are managed using Genie-2k software that is also used for spectrum display and processing. All spectra are recorded using 2048 channels, with a gain about 1 keV per channel in order to record photons in an energy range up to 2 MeV.

The SGS technique is applied to scan first for possible point sources by moving the detector along the drum axis. The segment containing the source is found from the count rate distribution at the maximum measured counts. At the segment of interest, the gamma projections are then recorded to reconstruct the image whose procedure is discussed later. The gamma-ray spectra are analyzed to determine the radioactive isotopes and their activities using the information obtained from the emission tomography. Gamma emission tomography images are reconstructed for the horizontal slices where the sources are found (see Fig. 1). The images are reconstructed using a filtered back-projection method and smoothed using intensity transformation and linear interpolation (Bruyant, 2002).

2.2. Monte Carlo simulation

The Monte Carlo-based PENELOPE software (Salvat et al., 2008) was used to investigate the response function and the full energy peak efficiency of the NaI(Tl) detector. The scintillation crystal of the detector is a cylinder of 76.2 mm diameter and 76.2 mm length supplied by Canberra, Company, US. In the simulation, the photomultiplier tube is replaced by an aluminum cylinder with 82.6 mm diameter and 30 mm length (Tam et al., 2015).

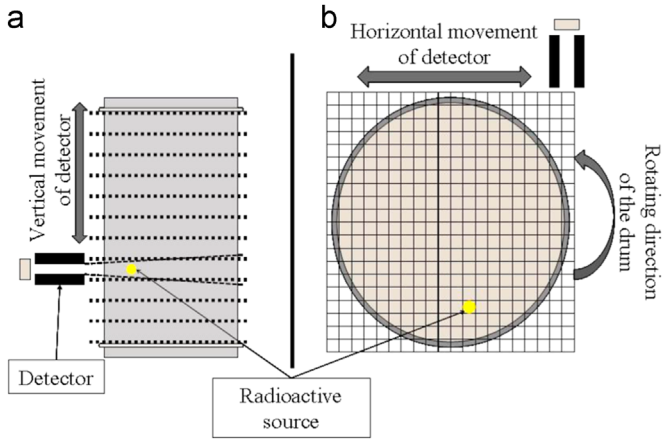

Fig. 1. Vertical movement of the detector along the waste drum (a), horizontal movement of the detector and the rotating direction of the waste drum (b).

PENELOPE performs simulations of coupled electron-photon transport in arbitrary materials. The PENMAIN routine was used to build a simulation model based on the geometry subroutine package PENGEOM, which performs particle tracking in material systems consisting of homogeneous regions (bodies) bounded by quadric surfaces. The full energy peak efficiency is obtained by multiplying the probability distribution function corresponding to the energy of interest (full-energy deposition) by the bin energy width:

$$\epsilon_P(E) = p_d.\, dE = \frac{N_p(E)}{N_s(E)} \quad (1)$$

where $\epsilon_P(E)$, p_d, dE, $N_p(E)$, $N_s(E)$ are respectively the full energy peak (FEP) efficiency derived from the simulation, the probability distribution function, the width of the energy bin, the number of the events recorded in the FEP and the number of photons emitted by the source (Thanh et al., 2013).

In the experiment, the spectrum peaks have a Gaussian form. However, the PENELOPE code does not simulate the physical processes of the broadening of the peaks. Therefore, to compare with experimental spectra, it is necessary to apply a Gaussian distribution to the simulated spectra. We developed a simple code for including resolution effect in gamma spectra from simulation. The FWHM function is defined by the following equation:

$$\mathrm{FWHM} = a + b\sqrt{E + cE^2} \quad (2)$$

The parameters $a = -0.0020$ MeV; $b = 0.0656$ MeV$^{1/2}$; $c = -0.0640$ MeV^{-1} are obtained by fitting FWHM function to the values of the experimental FWHM.

3. Results and discussion

3.1. Detection efficiency calibration

The aim is to compare a full energy peak efficiency computed with the PENELOPE software with the experimental data. The standard point sources were purchased from Eckert & Ziegler Isotope Products Company with relative combined uncertainties around 3%. Radionuclides used for measurement are ^{54}Mn, ^{60}Co, ^{65}Zn, ^{109}Cd, ^{133}Ba, ^{137}Cs, and the source activities are between 37.41 kBq and 39.96 kBq. The sources are placed on a Plexiglas® holder at 20 cm from detector window. The experimental efficiency values are obtained with relative combined uncertainties ranging from 3.1% to 5.5%. Full energy peak efficiencies are compared with those from PENELOPE in Table 1 and show a maximum deviation of 5.3% for all energies.

Table 1
Experimental and simulated values of full energy peak efficiency, their uncertainty and relative deviations.

Nuclides	Energy (keV)	ε_e	$U\varepsilon_e$ (%)	ε_{PEN}	U_{PEN} (%)	$\frac{\lvert\epsilon_{PEN}-\epsilon_e\rvert}{\epsilon_e}\times 100\%$
^{133}Ba	81.00	5.99E−03	3.2	5.93E−03	1.2	1.0
^{109}Cd	88.03	5.82E−03	4.2	6.01E−03	1.7	3.3
^{133}Ba	356.01	4.91E−03	3.1	4.93E−03	0.7	0.3
^{137}Cs	661.66	3.01E−03	3.1	3.11E−03	0.5	3.3
^{54}Mn	834.85	2.45E−03	4.8	2.55E−03	0.5	4.3
^{65}Zn	1115.52	1.91E−03	5.5	2.01E−03	0.7	5.3
^{60}Co	1173.20	1.84E−03	3.2	1.92E−03	0.7	4.4
^{60}Co	1332.49	1.69E−03	3.2	1.72E−03	0.8	1.8

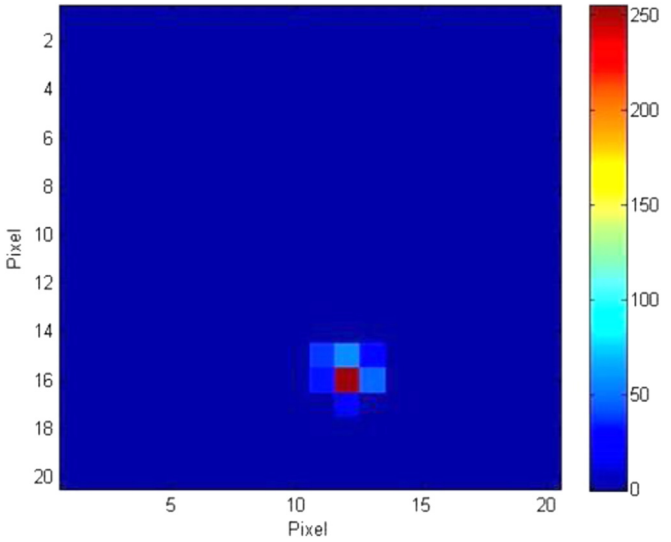

Fig. 2. Tomography image after detector effect deconvolution.

Table 2
The comparison between the source activities of ^{60}Co and ^{137}Cs with matrix air and sand respectively.

Nuclides	True activity (kBq)	Measured activity (kBq)	Matrix
^{60}Co	12.99(30)	13.36(26)	Air
^{137}Cs	37.37(111)	33.63(111)	Air
^{60}Co	12.99(30)	13.87(74)	Sand
^{137}Cs	37.37(111)	35.89(392)	Sand

Note: 12.99(30) = 12.99 ± 0.30.

3.2. Combination of the segmented gamma scanning and the gamma emission tomography

The test drum is divided into 11 segments and it is scanned from top to bottom. The peak position in the axial scan corresponds to the vertical position where the source is located. In this segment, the detector is then moved from left to right with a 3-cm step size. Next, the drum is rotated by an angle $\theta = 3^\circ$ and we record a next projection corresponding to the new angle. We obtain a set of projections after turning the waste drum around. It takes approximately 2 h to finish all scans for a single segment. We then reconstruct the tomography image (20×20 pixels) using the filtered back-projection method. Next, we estimate the Point Spread Function (PSF) of the imaging system by taking a row of data that goes through the source position (Maja, 2010). The detector effects are deconvoluted from the image using the acquired PSF (see Fig. 2).

By using both the segmented gamma scanning and the gamma emission tomography technique, we can calculate the X–Y-position of the source based on the reconstructed image. In the case studied, $(x_A, y_A) = (35 \pm 2, 14 \pm 2)$ (cm) while the real position is $(x_T, y_T) = (37 \pm 2, 12 \pm 2)$ (cm).

3.3. Validation of the source activity inside the waste drum

The activity of radionuclides monitored in this way can be calculated using the following equation:

$$A_i = \frac{N_P(E_i)}{\epsilon_P(E_i).\, I(E_i).\, t} \tag{3}$$

where A_i, $N_P(E_i)$, $\varepsilon_P(E_i)$, $I(E_i)$, t are the source activity (Bq), the full-energy peak net area, the relevant efficiency computed by the PENELOPE software using the source positions obtained from the emission tomography, the photon emission intensity corresponding to energy E_i and the acquisition live time (s), respectively.

The activity results of ^{137}Cs and ^{60}Co are presented in Table 2. The discrepancies between measured and true activities were smaller than 10% for both matrices.

4. Conclusion

The accuracy for locating the radioactive sources is improved by combining the segmented gamma scanning with the gamma emission tomography technique. The full energy peak efficiency and response function of the NaI(Tl) detector are then computed for the point source of the specified position. The measured activity shows a bias smaller than 10% for both air and sand matrices compared with the true activity of the radioactive source inside the waste drum.

Further investigation is required to account for multiple sources and to correct in combination with volume source and to correct for the attenuation and scattering of photons in a real waste drum, where the matrix is not always homogeneous.

Acknowledgments

This research is funded by Vietnam National Foundation for Science and Technology Development (NAFOSTED) under Grant number 103.04-2014.72.

References

Bai, Y.,F., Mauerhofer, E., Wang, D.,Z., Odoj, R., 2009. An improved method for the non-destructive characterization of the radioactive waste by gamma scanning. Appl. Radiat. Isot. 67, 1897–1903.
Bruyant, P.P., 2002. Analytic and iterative reconstruction algorithms in SPECT. J. Nucl Med. 43, 1343–1358.
Canberra, 2014. Osprey™–Universal Digital MCA Tube Base for Scintillation Spectrometry. ⟨http://www.canberra.com/products/radiochemistry_lab/pdf/Osprey-SS-C40303.pdf⟩.
Krings, T., Mauerhofer, E., 2011. Reconstruction of the activity of point sources for the accurate characterization of nuclear waste drums by segmented gamma scanning. Appl. Radiat. Isot. 69, 880–889.
Krings, T., Mauerhofer, E., 2012. Reconstruction of the isotope activity content of heterogeneous nuclear waste drums. Appl. Radiat. Isot. 70, 1100–1103.
Gurau, D., Sima, O., 2012. Simulation studies of the response function of a radioactive waste assay system. Appl. Radiat. Isot. 70, 305–308.
Maja, T.O., 2010. Tile-based Lucy-Richardson Deconvolution Modeling a Spatially-varying PSF for Fast Multiview Fusion of Microscopical Images, Technical Report 260. University of Freiburg, Germany.
Salvat, F., Fernández-Vaera, J.M., Sempau, J., 2008. PENELOPE-2008, A Code System for Monte Carlo Simulation of Electron and Photon Transport. Nuclear Energy Agency, Spain.
Tam, H.D., Chuong, H.D., Thanh, T.T., Nguyen, V.H., Trang, H.T.K., Tao., C.V., 2015. Advanced gamma spectrum processing technique applied to the analysis of scattering spectra for determining material thickness. J. Radioanal. Nucl. Chem. 303 (1), 693–699.
Thanh, T.T., Ferreux, L., Lépy, M.C., Tao., C.V., Pierre, S., 2013. Characterization of a cosmic suppression spectrometer. Appl. Radiat. Isot. 81, 114–118.